blood

Prepublished online December 20, 2013;
doi:10.1182/blood-2013-07-505099

Notch signals are required for in vitro but not in vivo maintenance of human hematopoietic stem cells and delay the appearance of multipotent progenitors

Patricia Benveniste, Pablo Serra, Dzana Dervovic, Elaine Herer, Gisele Knowles, Mahmood Mohtashami and Juan Carlos Zúñiga-Pflücker

Blood (print ISSN 0006-4971, online ISSN 1528-0020), is published weekly by the American Society of Hematology, 2021 L St, NW, Suite 900, Washington DC 20036.

Blood First Edition Paper, prepublished online December 20, 2013; DOI 10.1182/blood-2013-07-505099

Notch signals are required for *in vitro* but not *in vivo* maintenance of human hematopoietic stem cells and delay the appearance of multipotent progenitors

Patricia Benveniste[*#], Pablo Serra[*#], Dzana Dervovic[*#], Elaine Herer[‡], Gisele Knowles[#], Mahmood Mohtashami[*#], and Juan Carlos Zúñiga-Pflücker[*]

[*]Department of Immunology, University of Toronto, [#]Sunnybrook Research Institute, [‡]Women and Babies Program, Sunnybrook Health Sciences Centre

Correspondence: JC Zúñiga-Pflücker, Department of Immunology, University of Toronto, Sunnybrook Research Institute, 2075 Bayview Avenue, Toronto, ON, M4N 3M5, Canada. Email: jczp@sri.utoronto.ca

Running Title: Notch effect on human stem/progenitors cells

Key Points

- Notch signals expand human HSC ($CD90^{low}$) cells *in vitro* and delay the expansion of $CD45RA^{int}$ and $CD45RA^{hi}$ cells *in vitro*
- HSCs expanded *in vitro* are equal to *ex vivo* $CD90^{low}$ cells in immune-reconstitution

Summary

All blood cell lineages start from hematopoietic stem cells (HSCs), which were recently shown to represent a heterogeneous group of cells. In mice, Notch signaling promotes the maintenance of "stemness" as well as the expansion of self-renewing HSCs *in vitro*. Additionally, human $CD34^+$ cells were shown to expand *in vitro* in response to Notch signals. However, it is unclear whether Notch directly affects all HSCs, and whether this role is relevant *in vivo*. Here, we developed culture conditions that support the maintenance of $CD34^+CD133^+CD90^{low}CD38^-CD7^-CD10^-CD45RA^-$ ($CD90^{low}$) cells phenotypically-defined HSCs as well as two early progenitor cells $CD34^+CD38^-CD7^-CD10^-CD45RA^{int}$ (RA^{int}) and $CD34^+CD38^-CD7^-CD10^-CD45RA^{hi}$ (RA^{hi}) that were functionally equivalent to MPP-2 and LMPP, respectively, found in cord blood. Using a genetic approach, we show that Notch signals were required for HSC preservation, with cultured HSCs being equal to *ex vivo* HSC-cells in their ability to reconstitute immunodeficient mice; however, dnMaml-transduced HSCs were not maintained *in-vitro*. Interestingly, Notch signaling did not appear to be required for the self-renewal of human HSC *in vivo*. Our findings support the notion that Notch signals maintain human HSCs *in vitro* that have hematopoietic-reconstituting ability *in vivo* and delays the appearance of two new described early progenitor cells.

INTRODUCTION

The hematopoietic system has been conceptualized as operating within a hierarchical model, with the hematopoietic stem cell (HSC) at the apex[1]. Human umbilical cord blood (CB) $CD34^-$ cells would appear to be the most quiescent HSC capable of giving rise to $CD34^+CD90^{low}CD49f^+$ HSCs with long term reconstituting ability[2-4]. Whether HSCs are affected by Notch signaling remains controversial. For instance, Notch signaling does not appear to be required for the maintenance of adult HSCs in mice[5]. In contrast, Notch signaling was shown to play an important role in the expansion of self-renewing HSCs in vitro[6].

In humans, although a prominent role for Notch signaling is well documented based on the expansion of $CD34^+$ cells *in vitro*, which includes both HSCs and progenitor cells, no quantitative and functional direct comparison in the efficiency of reconstitution to fresh ex vivo HSCs has been reported[7-13]. Nonetheless, Notch appears to affect human HSCs, since $CD34^{-/+}$ HSCs were recently shown to have active Notch signaling. However, in contrast to the experimental approach used in mice, that shows that Notch is not required for HSC maintenance, no similar genetic manipulations have been reported for human HSCs[4,5].

Several human progenitors able to differentiate into lympho-myeloid cells have been found in CB and/or bone marrow (BM)[14-18]. Nevertheless, it remains difficult to establish a clear hierarchical structure starting from an HSC. We sought to address this by starting cultures with purified CB-derived HSCs and functionally defined intermediates to yield a composite and hierarchical relationship. We modified the OP9-DL1 cell co-culture system[19,20] to support the expansion of HSCs and made use of OP9 cells expressing two different levels of Delta-like-4 (Dll4)[21], therefore enabling the titration of Notch signaling on HSC. Additionally, using a genetic approach, we found that Notch signaling during the co-culture period was required for the maintenance of HSCs while delaying the appearance and frequency of downstream progenitors. However, *in vivo* competition experiments revealed that Notch signaling was not required for the maintenance of human HSCs within the BM.

Together, our findings support the notion that Notch signals can extend the period of time in which HSC function can be maintained *in vitro* by delaying the emergence of at least two early progenitors, which we have characterized here providing a more complete view of the early stages of human hematopoiesis.

METHODS

Umbilical cord blood samples

Human CB samples were obtained by syringe extraction and collected in a blood-pack unit containing citrate phosphate dextrose anti-coagulant (Baxter Healthcare, Deerfield, Illinois) from consenting mothers following delivery in accordance to approved guidelines established by the Research Ethics Board of Sunnybrook Health Sciences Centre. Within 24 hours of collection, cord blood mononuclear cells were isolated as previously described[19].

Mice

NOD.cg-Prkdc^{scid}IL2rg$^{tm/Wjl}$/Sz (NOD/SCID/γ_c^{null}, NSG) and Rag2$^{-/-}$ γ_c^{null} BALB/c mice were purchased from Jackson Laboratory (Bar Harbor, ME) and housed and bred in a pathogen-free facility. All animal procedures were approved by the Sunnybrook Health Science Centre Animal Care Committee.

Generation of OP9-Dll4

OP9-Ctrl, OP9-DL4^{hi} and OP9-DL4^{low} cells were generated and maintained as previously described[22].

Cord blood purification

Cord blood cells were lineage depleted using Stem-Sep human Progenitor Cell Enrichment kit (Stem cell technology) according to the manufacturer's protocol, and further purified as described in detail in the Supplemental Methods.

Cocultures

OP9-Ctrl, OP9-DL4^{hi} and OP9-DL4^{low} cells were plated and maintained as previously described[22-24], and used in cocultures as described in detail in the Supplemental Methods. For clonal analysis, sort deposited cells were cultured for an additional 14-21 days under T or myeloid conditions as described in detail in the Supplemental Methods.

In vivo reconstitutions

Donor cells were sorted for the indicated markers and then injected intrahepatically into neonatal immune-deficient mice irradiated with 2 Gy. After 10 weeks mice were sacrificed and thymus, bone marrow and spleen were analyzed by flow cytometry. Details of the cells used and analysis are described in the Supplemental Methods.

dnMaml construct and retroviral transductions

The sequence encoding for amino acids 8-74 from mouse *Mastermind like 1* (Maml1) gene was fused, in frame, to a 5'-eGFP sequence using described cloning methods. This dominant-negative form of MAML1 (dnMaml) was then cloned into retroviral or lentiviral vectors to be used for transduction experiments of CB cells as described in detail in the Supplemental Methods.

Precursor-Product relationships

In vitro derived $CD45RA^{int}$ cells were sorted on day 18 from cultures, on OP9-$Dl4^{hi}$-$DL4^{low}$ or -Ctrl. Sorted cells (10,000 cells) were then cultured again on the OP9 cells they were derived from, in Stem. After 2 and 3 days, analysis of CD45RA expression on gated $CD34^{+}CD38^{-}CD7^{-}CD10^{-}$ cells was performed.

qPCR analysis

Total RNA was isolated in Trizol-reagent and reverse transcribed using Superscript-III and Oligo(dT) primers (Invitrogen). Diluted cDNA samples from cultures were used as described in detail in the Supplemental Methods.

Statistical Analysis:

T-test unpaired and paired two-tailed test was performed using Excel software, and prism software.

RESULTS

Characterization of early hematopoietic subsets in cord blood

We have used CB to identify early hematopoietic subsets using previously described markers[2,25], with the addition of Rhodamine-123 (Rho) and CD133 to further characterize human HSC- and multipotent progenitor (MPP)-subsets. Analysis of CD45RA expression from Lin^-CD135^+ cells showed the presence of three populations, with the most abundant fraction being $CD45RA^-$. As shown in Figure 1A, the $CD45RA^-$ fraction ($CD45RA^-$ cells) was further analyzed for CD133 expression and Rho uptake, and we identified the HSC fraction as having a $CD90^{low}$ phenotype, which was found only in the $CD45RA^-CD133^+CD135^+Rho^{low}$ fraction. Not surprisingly, $CD90^-$ cells made up the vast majority of the Rho^{low} subset, likely corresponding to an MPP-enriched subset. $CD135^+CD45RA^-CD133^+Rho^{low}CD90^{low}$ cells, which were also $CD38^{low}CD7^-CD10^-$ (not shown), hereafter referred to as HSCs, were used in subsequent experiments.

Cocultures with a modified OP9 system for HSC expansion

To examine how Notch signals could influence the CB HSC fraction, these cells were cultured on OP9-Ctrl cells (GFP alone) or on OP9 cells expressing different levels of Dll4 (OP9-$DL4^{low}$ and OP9-$DL4^{hi}$)[21] (Fig. S1C), together with cytokines[3,26] to support survival and expansion of HSCs and early progenitors. Co-cultures were analyzed on a weekly basis for the expression of markers that define HSCs. By day 21, we noted that co-cultures grown on OP9-$DL4^{hi}$ and -$DL4^{low}$ cells displayed a greater frequency of $CD34^+$ cells than those on OP9-Ctrl cells (Fig. 1B). An additional and expected effect of Notch signaling was the generation of $CD34^+CD7^+$ cells, early T-lineage cells[19], present in $DL4^{hi}$ and $DL4^{low}$ co-cultures starting with either HSCs or MPPs, but not seen in the absence of Dll4 (Ctrl) (Fig. S1D).

Based on these observations, we looked specifically at $CD34^+CD7^-$ cells at different time points, and found that CD45RA and CD38 were expressed at different levels and in different proportions on $CD34^+CD7^-$ gated cells (Fig. 1C). In particular, the $CD45RA^-$ and $CD45RA^{int}$ subsets were clearly present in cultures grown on $DL4^{hi}$ but not in Ctrl,

while the CD45RA^{hi} subset was abundantly present in co-cultures lacking Notch signaling (Ctrl).

Since co-cultures initiated with HSCs under Notch signaling conditions contained a substantial fraction CD45RA^{-} cells, we analyzed whether CD90^{low} cells were present after 3 weeks. Figure S1E shows CD90^{low} cells only in DL4^{hi} and DL4^{low} cultures but not in OP9-Ctrl cultures, nor in cultures initiated with downstream CD90^{-} cells (Fig. S1F).

We calculated the expansion of CD45RA^{-} (CD133^{+}CD34^{+}CD38^{-}CD7^{-}CD45RA^{-}) cells, and phenotypically-defined HSCs (pHSCs) as (CD133^{+}CD34^{+}CD38^{-}CD7^{-}CD45RA^{-} CD90^{low}) based on the absolute cellularity recovered from the starting HSCs (Fig. 2A). CD45RA^{-} and PHSCs cultured on Ctrl expanded minimally (Fig. 2A, B). However, when cultured with DL4^{hi}, CD45RA^{-} and pHSCs expanded 6-12 and 2-4 fold after 2-3 weeks, respectively (Fig. 2A-B). A smaller, but significant, expansion was also seen with DL4^{low}. Similar data were obtained when OP9-DL1^{hi} cells were used (data not shown). These results suggest that a high or low level of Notch signaling retards differentiation of pHSCs, allowing for some cellular expansion. We conclude that the modified OP9-DL4 co-culture system appears to maintain cells that are phenotypically identical to the input HSCs.

***In vivo* potential of HSCs generated *in vitro*:**

Although phenotypically-defined HSCs were maintained and expanded in the presence of Notch signals *in vitro,* the functional potential of these cells remained to be verified. We therefore compared the capacity of isolated DL4^{hi} derived d14 ($2x10^{3}$) pHSCs with that of 25-fold more phenotypically-defined MPP (CD90^{-}) (pMPP) cells, isolated in parallel DL4^{hi} derived d14 ($5x10^{4}$), to repopulate sublethally-irradiated NOD/SCID/γ_c^{null} (NSG) mice.

After ten weeks, BM samples from pHSC and pMPP reconstituted mice contained macrophages (CD33^{+}CD14^{+}), granulocytes (CD33^{+}CD15^{+}), and lymphoid cells (CD19^{+} B- or CD7^{+} T-cells) (Fig. 2C-D). In all 8 mice were analyzed in two groups of four (Fig. 2E), and absolute numbers of myeloid or lymphoid cells were similar between the two

groups. Therefore both cultured pHSC and pMPP cells have lympho-myeloid reconstitution potential.

We next wanted to compare d14 *in vitro*-grown pHSCs with freshly isolated HSCs for their ability to repopulate immune-deficient mice. NSG mice were injected with fresh HSCs ranging from 0.5-3x10^3 cells/mouse, and the resulting expansion of CD45RA$^-$ cells after 10 weeks within the BM of host mice was used to determine the expected cellular yield from injected HSCs (Fig. 2F). A linear relationship was observed with the absolute number of donor CD45RA$^-$ cells in the BM correlating directly with the number of injected HSCs. We then extrapolated the number of CD45RA$^-$ cells recovered from mice injected with 2x10^3 d14 *in vitro*-grown pHSCs and found that this corresponded to the equivalent of 0.5x10^3 freshly isolated HSCs, or a ~0.25x equivalency in cellular outcome (Fig. 2F). In contrast, very few CD45RA$^-$ were found in mice injected with pMPP cells, even though x25 fold more cells were injected. We conclude that pHSCs cultured in the presence of Notch signaling act as SCID-mouse repopulating cells (SRCs)[27] similar to freshly isolated HSCs.

Effect of Notch inhibition on the maintenance/expansion of HSC and/or CD45RA$^-$ subsets derived *in vitro*.

To test whether the *in vitro* expansion of pHSC and/or CD45RA$^-$ cells is regulated by canonical Notch signaling, we transduced *ex vivo* HSCs with the dnMaml-GFP construct[5] to prevent cells from responding to Notch signals. HSCs cells expressing dnMaml-GFP and/or control YFP were generated and cultured on Ctrl, DL4^{hi} and DL4^{low} cells for an additional 2-3 weeks. Analysis of CD34$^+$CD38$^-$CD7$^-$ gated cells from Ctrl cultures showed no CD45RA$^-$, and therefore no CD90^{low} cells, few CD45RA^{int}, and a majority were CD45RA^{hi} cells, regardless of the presence or the absence of dnMaml (Fig. 3A last two columns). In sharp contrast, in CD34$^+$CD38$^-$CD7$^-$ gated cells derived from DL4^{hi} cultures expression of dnMaml-GFP totally abrogated the maintenance of both CD45RA$^-$ cells and CD90^{low} cells, and accelerated the progression to the CD45RA^{int} and CD45RA^{hi} stages. Similar results were observed in DL4^{low} cultures expressing the dnMaml-GFP construct.

These results point to Notch signaling as being necessary for the maintenance of $CD45RA^{-}$ and $CD90^{low}$ cells; in its absence, differentiation proceeds with the accelerated appearance of both $CD45RA^{int}$ and $CD45RA^{hi}$ stage cells. Additionally, cellular expansion of $CD45RA^{-}$ cells is dependent upon Notch signaling, as the fold expansion of YFP-only transduced cells relative to d7, was greatest in $DL4^{hi}$ cocultures, while not being evident in dnMaml-Ctrl transduced cells (Fig. 2B).

Is Notch signaling required for the maintenance/expansion of HSCs *in vivo*?

We next tested whether this effect was also the case *in vivo* using competitive transplantation experiments. Equivalent numbers of sorted HSC expressing either dnMaml-GFP^{+} or YFP^{+} were injected into sublethally irradiated neonatal NSG mice. Ten weeks later, the contribution of GFP and/or YFP expressing cells was analyzed in BM, thymus and spleen. As shown in Figure S2A (left panels), the BM and spleen contained $CD45^{+}$ donor cells, which included GFP^{+} and YFP^{+} cells. In both donor types, myeloid and B-lymphoid cells were similarly observed. Analysis of the BM from ten independently reconstituted mice is shown in Figure S2D-G. Similar results were found in the spleen.

Analysis of the thymus showed $CD45^{+}$ donor cells, but composed nearly entirely of YFP^{+} cells, with very few GFP^{+} cells (Fig. S2B). The YFP^{+} cells included mainly T cells that expressed high levels of CD3. These findings clearly demonstrate effective abrogation of Notch signaling in GFP^{+} cells. To test the critical question of whether Notch signaling plays any role in the maintenance and/or self-renewal of human HSCs (SRC) *in vivo*, absolute numbers of donor-derived $CD45RA^{-}$ and pHSCs were compared in the BM, and were found similar in dnMaml-GFP and YFP injected mice (Fig. 3C,D-E). These results strongly suggest that Notch inhibition did not have an effect on the maintenance and/or self-renewal of SRCs within the BM microenvironment.

Effect of Notch engagement on the expansion of CD45RA subsets derived *in vitro*

We next examined the consequences of the Notch-driven expansion of HSCs, on early progenitors, namely $CD45RA^{int}$ and $CD45RA^{hi}$ fraction (as shown in Fig. 1C). We calculated the expansion of each progenitor fraction at weekly intervals based on the absolute number of cells recovered. Figure 4A shows that both $CD45RA^{int}$ and $CD45RA^{hi}$

fractions expanded the most in the absence of Notch signals (Ctrl). In the presence of Notch signaling, the generation of CD45RA^{int} and CD45RA^{hi} cells was not favored in particular with DL4^{hi} (Fig. 4; middle panels). These data suggest that a high or low level of Notch signaling expands CD45RA^{-} and pHSCs, maintains them in an undifferentiated state, and restrains their differentiation into both CD45RA^{int} and CD45RA^{hi} progenitors.

Precursor-product relationship of CD45RA fractions derived *in-vitro*.

We next determined precursor-product relationships between CD45RA^{int} and CD45RA^{hi} fractions generated *in vitro.* CD45RA^{int} were sorted from d21 Ctrl, DL4^{hi} and DL4^{low} co-cultures and then re-cultured (new d0) under the same conditions from which they were originally derived. As shown in Figure 4B, more than 80% of CD45RA^{int} became CD45RA^{hi} after only 2 days of further culture on Ctrl or DL4^{low}, but cells progressed more slowly to CD45RA^{hi} when re-cultured in the presence of a high Notch signal. This indicated that CD45RA^{int} were precursors of CD45RA^{hi} cells. We concluded that CD45RA^{-} give rise to CD45RA^{int} and then to CD45RA^{hi}, with Notch signaling restraining this developmental progression.

Functional characterization of progenitor cells: Bulk and clonal assays

We next addressed the differentiation potential of CD45RA^{int} and CD45RA^{hi} subsets and examined their ability to generate CFU in methyl-cellulose cultures. Figure 5A (top left panels) shows that CD45RA^{int} cells derived from either Ctrl or DL4^{low} cultures gave rise to BFU-E, GM, G and M colonies. In striking contrast, very few if any BFU-E colonies were found in the CD45RA^{hi} fraction from OP9-DL4^{low} or -Ctrl cultures. Nevertheless, CD45RA^{hi} cells have clear myeloid potential in that they gave rise to GM, G and M colonies at higher frequencies than *ex vivo* MPP cells (Fig. 5A). Therefore, CD45RA^{int} and CD45RA^{hi} cells both possess myeloid potential but CD45RA^{hi} cells appear to have lost erythroid potential.

As shown in Figure S1A, a similar CD45RA^{int} subset is present in CB cells, which are CD45RA^{int}CD135^{+}CD133^{+}CD7^{-}CD10^{-}Rho$^{low/int}$ (*ex vivo* CD45RA^{int}). By comparing the myeloid potential of *in vitro* derived CD45RA^{int} cells to *ex vivo* CD45RA^{int} cells, we

observed that both CD45RA^{int} cells display erythro-myeloid potential (Fig. 5A, third top panel). To further characterize the BFU-E potential within this population, we fractionated *ex vivo* CD45RA^{int} cells into Rho^{low} and Rho^{int} fractions as shown in Figure S1A and tested each fraction separately. Only the Rho^{int} fraction gave rise to BFU-E although both fractions generated GM, G and M CFU colonies (Fig. 5B).

The lymphoid potential of CD45RA^{int} and CD45RA^{hi} cells generated *in vitro* was also assessed. The ability to generate T and B- cells was observed in both CD45RA^{int} (Fig. 5C) and CD45RA^{hi} cells (Fig. 5D). The comparison of *in vitro* CD45RA^{int} to *ex vivo* CD45RA^{int} revealed that *ex vivo* CD45RA^{int} also had T and B-lineage potential (Fig. 5C). However, a lower frequency of B cells was consistently found as compared to *in vitro* derived CD45RA^{int} cells. When *ex-vivo* derived CD45RA^{int} Rho$^{low/int}$ cells were further fractionated into Rho^{low} and Rho^{int} cells, almost no B cells were generated in the Rho^{int} fraction whereas the Rho^{low} fraction did give rise to B cells (Fig. 5E).

To define the potential of these fractions at the clonal level, we repeated these analyses under limiting dilution conditions. We found that every single clone of CD45RA^{int} and CD45RA^{hi} was able to generate T cells regardless of the presence or absence of Notch signaling during the first 3 weeks of culture. Interestingly, T cells were also generated from *ex vivo* CD45RA^{int} clones at a similar frequency (Fig. 5B, S3A, Tables S1, S2). Additionally, B cells as well as macrophages and granulocytes (Fig. S3, Tables S1, S2), were also present at comparable frequencies from d21 co-cultures clonally sorted CD45RA^{int} and CD45RA^{hi} cells.

Since the majority of CD45RA^{int} or CD45RA^{hi} clonal outcomes contained both CD19^{+} cells and CD33^{+} cells (Table S3) and given the T cell frequencies observed (Table S2), our clonal analysis indicates that both CD45RA^{int} and CD45RA^{hi} cells were able to give rise to T, B, and myeloid cells. Therefore, a substantial fraction of both CD45RA^{int} and CD45RA^{hi} cells are lympho-myeloid precursors the former compatible with an MPP.2 type of cell and the latter with a lymphoid-primed multipotent progenitor (LMPP) type of cell[28].

Ex vivo CD45RA^{int}Rho^{low} cells have a similar potential to *in vitro* generated CD45RA^{hi} cells (Fig. S5). Therefore *ex vivo* derived CD45RA^{int}Rho^{low} cells are LMPP-like cells. However, ex *vivo* CD45RA^{int}Rho^{int} cells have the potential to generate at the clonal level GM, G, M and T cells (Tables S1, S2). Only a fraction of them also have *in vitro* erythroid potential. So at least two subsets are present in *ex vivo* CD45RA^{int} cells, a minority subset with erythro-myeloid and lymphoid potential and a majority subset with myeloid and T cell potential, but devoid of B and erythroid potential *in vitro*.

Molecular characterization of CD45RA subsets

To further characterize the *in vitro* generated CD45RA^{int} and CD45RA^{hi} cells, we performed a qPCR analysis. Figure 6 shows that *DTX1 (Deltex1)* was expressed only on CD45RA^{int} and CD45RA^{hi} cells grown from DL4^{low} cultures (top left panel) consistent with Notch signaling in these cultures. *GATA1* and *GATA2* transcripts were expressed in CD45RA^{int} cells but were present at low levels in CD45RA^{hi} cells. *GATA1* expression was high in CD45RA^{int} cells from DL4^{low} cultures, which possessed a higher BFU-E frequency.

On the other hand, *IKZF1* (*Ikaros*) transcripts were expressed at higher levels in CD45RA^{hi} cells from either Ctrl or DL4^{low} cultures. This, together with the low levels of *GATA1*, confirmed a similar pattern of expression to that of mouse cells with similar differentiation potential. Additionally, *SPI1* (*PU.1*), *HOXB2*, *MLL3* and *TAL1* (*SCL*) (Fig. 6) were expressed at higher levels in CD45RA^{int} than in CD45RA^{hi} cells from either Ctrl or DL4^{low} cultures, correlating with their earlier stage of differentiation. Taken together, the gene expression patterns found in both lympho-myeloid progenitors generated *in vitro* correspond to the pattern of gene expression predicted from their differentiation potential.

***In vivo* potential of *in vitro*-generated CD45RA^{int} and CD45RA^{hi} and *ex vivo* CD45RA^{int} cells.**

We next assessed the *in vivo* developmental potential of *in vitro* CD45RA^{int} and CD45RA^{hi} cells and *ex vivo* CD45RA^{int} cells to reconstitute BM and thymi of BALB/c

Rag$^{-/-}\gamma_c^{null}$ mice. A relatively low number (10^5) of CD45RA^{int} and CD45RA^{hi} cells from DL4^{low} or Ctrl cultures (2-4 weeks) were injected into immune-deficient neonatal mice. CD45RA^{int} and CD45RA^{hi} cells isolated from DL4^{low} cultures engrafted mice with donor CD45$^+$ cells in the BM and thymus, including B and myeloid cells in the BM and T cells in the thymus, respectively, when analyzed 4 to 7 weeks post injection (Fig. 7A, B, D). We noted different frequencies of CD4$^+$CD8$^-$ cells, which are mainly immature single positive cells, reflect the different temporal kinetics of reconstitution from the CD45RA^{int} and CD45RA^{hi} cells.

In contrast, mice injected with similar numbers of CD45RA^{int} and CD45RA^{hi} cells from Ctrl cultures were unable to effectively reconstitute the thymus, although they did reconstitute BM, with B and myeloid cells (Fig. 7A, B). Notably, high levels of CD45$^+$ engraftment were seen in the thymus of 15 mice injected with CD45RA^{int} from DL4^{low} cultures as compared to 7 mice injected with CD45RA^{int} from Ctrl cultures (Fig.7D). Nonetheless, injection of higher numbers of these populations enabled CD45RA^{int} and CD45RA^{hi} cells from Ctrl cultures to reconstitute the thymus (data not shown). Thus, it appears that Notch signaling facilitated but was not required for thymic reconstitution. Lastly, e*x vivo* CD45RA^{int} cells engrafted both the bone marrow (B and myeloid cells) and thymus (Fig. 7 C). Results from 7 independent mice are presented in Fig. 7D.

DISCUSSION

We have defined culture conditions suitable for the maintenance of human HSCs, thus allowing us to directly test the effects of Notch signaling on prospectively defined HSCs. Here, we have found that HSCs are specifically affected by Notch signals *in vitro*, but do not rely on Notch signals for their expansion *in vivo*. In addition, our culture system enabled us to identify and characterize two new early progenitors, functionally akin to MPP-2 ($CD45RA^{int}$) and LMPP ($CD45RA^{hi}$) cells that were also found in CB.

The role of Notch on HSCs remains controversial. In aggregate, our current understanding points to a dichotomy in the role of Notch in HSC expansion: *In vitro* systems support a role for both mouse HSCs[6] and human $CD34^+$ cells[4,7,8,10,29] while *in vivo* approaches discounted a role for mouse HSCs[5]. Mechanisms of how Notch signaling influence the maintenance and expansion of human HSCs *in vitro* versus *in vivo* are complex and difficult to dissect since they require discrete fractionation of the different HSC subsets[4,30].

As described by Anjos-Afonso[4], both the most primitive quiescent HSC ($CD34^-$) and its progeny $CD34^+CD90^{low}CD49f^+$ express *DTX1* and *HES1*, display different kinetics of reconstitution, and appear to be affected differentially upon Notch inhibition *in vivo.* Although a pharmacological inhibitor of Notch was used in this report, which is known to affect other non-hematopoietic tissues, maintenance and self-renewal of the $CD34^-$ subset was affected *in vivo*[4]. However, here we show that competitive transplantation experiments using dnMaml for Notch inhibition in HSCs possessed equal reconstitution abilities *in vivo*, consistent with the results in mice[5]. Nevertheless, whether loss of Notch signaling affected the temporal kinetics of reconstitution, as seen in mice[31], was not addressed.

Our results not only serve to extend the findings from Bernstein and colleagues[7], but more importantly, we now show that in culture HSCs are an important target of Notch signals. Additionally, it appears that cells at an early stage, $CD34^+CD38^-CD7^-CD10^-CD45RA^-$ cells ($CD45RA^-$), are maintained and expanded in the presence of Notch signals. Thus, by clarifying the target population exposed to Notch signals, a clearer picture of which cells are affected by this pathway has emerged.

A mechanism for how Notch signaling influences the maintenance and expansion of human HSCs *in vitro* is likely to involve several pathways regulated by Notch targets, such as cMyc, Cdkn1, and PTEN, all of which have been shown to affect HSC expansion/maintenance[32,33]. However, the dichotomy between the requirements for Notch *in vitro* versus its dispensable role *in vivo* is likely due to the complex nature of the BM niche, in which Notch signals may be only one of many factors[17,34,35], while *in vitro* it becomes critically important. By removing HSCs from their normal BM niche, these cells, would require a strong Notch signaling *in vitro* to compensate for the absence of the other signaling queues (Fig. S4A).

We also showed that both *in vitro*-derived phenotypically-defined HSC ($CD45RA^-$ $CD90^{low}$) and phenotypically-defined MPP ($CD45RA^-CD90^-$) populations were multipotent. However, upon transfer in to mice, *in* vitro grown pHSCs were about 200 times more effective in generating $CD45RA^-$ cells than pMPPs, probably due the fact that only $CD90^{low}$ cells were able to self-renew *in vivo*. In this regard, we found that *in vitro*-derived pHSCs approximated the SRC-activity of freshly-isolated HSCs when directly compared. Given the variability associated with *in vivo* manipulations, the use of a xenogeneic model system, and the relatively low numbers of cells injected, we can estimate that the two populations are likely similar in function.

The immediate stages following the differentiation of human CB HSC are not fully appreciated, nor are the precursor–product relationships between these early progenitors clearly established. We now show that Notch signaling appears to delay the differentiation of $CD45RA^-$ cells *in vitro*, as the appearance of downstream $CD45RA^{int}$ and $CD45RA^{hi}$ cells is inhibited by Notch signals. We next characterized and showed that $CD45RA^-$ cells gave rise to $CD45RA^{int}$, then to $CD45RA^{hi}$ and then to $CD45RA^{hi}$ ($CD10^+$) cells (manuscript in preparation) *in vitro*, following a progression in which each fraction of lympho-myeloid progenitors corresponds to a more differentiated stage of development.

$CD45RA^{int}$ cells obtained *in vitro* were shown at both population and clonal levels, and at the transcript level, to be functionally equivalent to phenotypically defined multipotent cells (pMPP-2), whereas the $CD45RA^{hi}$ cells qualify as LMPP-like cells. Both subsets

were able to reconstitute the same lympho-myeloid lineages when injected into immune-deficient mice. Interestingly both subsets could reconstitute the thymus of immune-deficient mice, but when these *in vitro* cells had received Notch signals thymic reconstitution was greatly facilitated. In the absence of Notch signaling, thymic reconstitution occurs but only when higher numbers of cells are injected. So Notch signals facilitate but are not required for thymic reconstitution. Similar functional subsets were characterized in CB (*ex vivo* CD45RA^{int}). The presence of a weak erythroid differentiation potential in *ex vivo* Rho^{int} CD45RA^{int} suggests that this phenotypically defined subset of CB cells could include both MPP-2 and GMP precursor cells[36,37]. Interestingly, *ex vivo* CD45RA^{int}Rho^{low} cells lacked erythroid potential, but had myeloid and lymphoid potential *in vitro*. Therefore, both subsets of *ex vivo* CD45RA^{int} cells, Rho^{int} and Rho^{low}, would appear to include cells that qualify as MPP-2 and LMPP, respectively.

Hao *et al.*[16] reported, at the clonal level, a Lin^{-} CD34^{+}CD7^{-} early thymic lympho-myeloid precursor that has erythro-lympho-myeloid potential, a finding unique to human. The presence of thymic progenitors with such a potential correlates well with our *in vitro*-generated CD45RA^{int}, as well as with *ex vivo* CD45RA^{int} cells. *Ex vivo* CD45RA^{int}Rho^{low} cells, described here as LMPP-like cells are at a more immature stage of differentiation than the cells recently described by Kohn *et al.*[18], in that they possess GM and G myeloid potential and express CD45RA at only intermediate levels. Haddad *et al.*[14] characterized in CB an *ex vivo* CD34^{+}CD45RA^{hi} cell, described as progeny of the *in vitro* derived CD45RA^{int} subset that shares characteristics with our *in vitro* generated CD45RA^{hi} subset.

The model presented in Fig. S4B summarizes our findings. The human hematopoietic hierarchy appears similar to the murine system except for the fact that unlike the murine system, human pMPP-like cells with erythroid potential are able to reconstitute the thymus. We showed that the Notch-dependent maintenance of human pHSCs leads to an arrest in the differentiation of each of the lympho-myeloid progenitors (MPP-2 and LMPP) derived from it.

ACKNOWLEDGEMENTS

We thank Drs. Richard Miller and Norman Iscove for helpful discussion and critical review of the manuscript. We also thank Dr. Els Verhoeyen for helpful technical advise on the generation and concentration of lentiviral supernatants. We would like to acknowledge Courtney McIntosh for their expertise in cell sorting and Roxanne Holmes, John Xu and Sanam Taheri for their technical support. We are grateful to Dr. Rose Kung and staff of the Women and Babies program at Sunnybrook Health Sciences Centre for their ongoing support in providing us with umbilical cord blood.

This work was supported by grants to JCZP from the Terry Fox Foundation (TFF-15005) Canadian Institutes of Health Research (CIHR, MOP-119538 and HOP-83070) and The Krembil Foundation.

AUTHORSHIP

P.B. and P.S. performed and designed the research. M.M and D.D generated the OP9-DL4 lines. E.H provided the umbilical cord blood samples. G.C.K performed the flow cytometric cell sorts. P.B. and J.C.Z.P wrote the paper.

CONFLICT OF INTEREST

We declare no competing financial interests

REFERENCES

1. Kondo M, Wagers AJ, Manz MG, et al. Biology of hematopoietic stem cells and progenitors: implications for clinical application. *Annu Rev Immunol*. 2003;21:759-806.

2. Majeti R, Park CY, Weissman IL. Identification of a hyerarchy of multipotent hematopoietic progenitors in human cord blood. *Cell Stem Cell*. 2007;1(6):635-645.

3. Notta F, Doulatov S, Laurenti E, Poeppl A, Jurisica I, Dick JE. Isolation of single human hematopoietic stem cells capable of long-term multilineage engraftment. *Science*. 2011;333(6039):218-221.

4. Anjos-Afonso F, Currie E, Palmer HG, Foster KE, Taussig DC, Bonnet D. CD34(-) cells at the apex of the human hematopoietic stem cell hierarchy have distinctive cellular and molecular signatures. *Cell Stem Cell*. 2013;13(2):161-174.

5. Maillard I, Koch U, Dumortier A, et al. Canonical notch signaling is dispensable for the maintenance of adult hematopoietic stem cells. *Cell Stem Cell*. 2008;2(4):356-366.

6. Butler JM, Nolan DJ, Vertes EL, et al. Endothelial cells are essential for the self-renewal and repopulation of Notch-dependent hematopoietic stem cells. *Cell Stem Cell*. 2010;6(3):251-264.

7. Delaney C, Heimfeld S, Brashem-Stein C, Voorhies H, Manger RL, Bernstein ID. Notch-mediated expansion of human cord blood progenitor cells capable of rapid myeloid reconstitution. *Nat Med*. 2010;16(2):232-236.

8. Gammaitoni L, Bruno S, Sanavio F, et al. Ex vivo expansion of human adult stem cells capable of primary and secondary hemopoietic reconstitution. *Exp Hematol*. 2003;31(3):261-270.

9. Piacibello W, Sanavio F, Garetto L, et al. Extensive amplification and self-renewal of human primitive hematopoietic stem cells from cord blood. *Blood*. 1997;89(8):2644-2653.

10. Ohishi K, Varnum-Finney B, Bernstein ID. Delta-1 enhances marrow and thymus repopulating ability of human CD34(+)CD38(-) cord blood cells. *J Clin Invest*. 2002;110(8):1165-1174.

11. Androutsellis-Theotokis A, Leker RR, Soldner F, et al. Notch signalling regulates stem cell numbers in vitro and in vivo. *Nature*. 2006;442(7104):823-826.

12. Delaney C. V-FB, Aoyama K., Brashem-Stein C., and irwin D. Bernstein. Dose-dependent effects of the Notch ligand Delta1 on ex vivo differentiation and in vivo marrow repopulating ability of cord blood cells. *Blood* 2005;106(8):2693-2699.

13. Dahlberg A, Delaney C, Bernstein ID. Ex vivo expansion of human hematopoietic stem and progenitor cells. *Blood*. 2011;117(23):6083-6090.

14. Haddad R, Guardiola P, Izac B, et al. Molecular characterization of early human T/NK and B-lymphoid progenitor cells in umbilical cord blood. *Blood*. 2004;104(13):3918-3926.

15. Haddad R, Guimiot F, Six E, et al. Dynamics of thymus-colonizing cells during human development. *Immunity*. 2006;24(2):217-230.

16. Hao QL, Zhu J, Price MA, Payne KJ, Barsky LW, Crooks GM. Identification of a novel, human multilymphoid progenitor in cord blood. *Blood*. 2001;97(12):3683-3690.

17. Doulatov S, Notta F, Laurenti E, Dick JE. Hematopoiesis: a human perspective. *Cell Stem Cell*. 2012;10(2):120-136.

18. Kohn LA, Hao QL, Sasidharan R, et al. Lymphoid priming in human bone marrow begins before expression of CD10 with upregulation of L-selectin. *Nat Immunol*. 2012;13(10):963-971.

19. Awong G, Herer E, Surh CD, Dick JE, La Motte-Mohs RN, Zuniga-Pflucker JC. Characterization in vitro and engraftment potential in vivo of human progenitor T cells generated from hematopoietic stem cells. *Blood*. 2009;114(5):972-982.

20. La Motte-Mohs RN, Herer E, Zúñiga-Pflücker JC. Induction of T-cell development from human cord blood hematopoietic stem cells by Delta-like 1 in vitro. *Blood*. 2005;105(4):1431-1439.

21. Mohtashami M, Shah DK, Nakase H, Kianizad K, Petrie HT, Zuniga-Pflucker JC. Direct comparison of Dll1- and Dll4-mediated Notch activation levels shows differential lymphomyeloid lineage commitment outcomes. *J Immunol*. 2010;185(2):867-876.

22. Schmitt TM, Zuniga-Pflucker JC. Induction of T cell development from hematopoietic progenitor cells by delta-like-1 in vitro. *Immunity*. 2002;17(6):749-756.

23. Awong G, La Motte-Mohs RN, Zuniga-Pflucker JC. Generation of pro-T cells in vitro: potential for immune reconstitution. *Semin Immunol*. 2007;19(5):341-349.

24. Awong G, La Motte-Mohs RN, Zuniga-Pflucker JC. In vitro human T cell development directed by notch-ligand interactions. *Methods Mol Biol*. 2008;430:135-142.

25. Park CY, Majeti R, Weissman IL. In vivo evaluation of human hematopoiesis through xenotransplantation of purified hematopoietic stem cells from umbilical cord blood. *Nat Protoc*. 2008;3(12):1932-1940.

26. Benveniste P, Frelin C, Janmohamed S, et al. Intermediate-term hematopoietic stem cells with extended but time-limited reconstitution potential. *Cell Stem Cell*. 2010;6(1):48-58.

27. Sirard C, Lapidot T, Vormoor J, et al. Normal and leukemic SCID-repopulating cells (SRC) coexist in the bone marrow and peripheral blood from CML patients in

chronic phase, whereas leukemic SRC are detected in blast crisis. *Blood*. 1996;87(4):1539-1548.

28. Adolfsson J, Mansson R, Buza-Vidas N, et al. Identification of Flt3+ lympho-myeloid stem cells lacking erythro-megakaryocytic potential a revised road map for adult blood lineage commitment. *Cell*. 2005;121(2):295-306.

29. Carlesso N, Aster JC, Sklar J, Scadden DT. Notch1-induced delay of human hematopoietic progenitor cell differentiation is associated with altered cell cycle kinetics. *Blood*. 1999;93(3):838-848.

30. Yamamoto R, Morita Y, Ooehara J, et al. Clonal analysis unveils self-renewing lineage-restricted progenitors generated directly from hematopoietic stem cells. *Cell*. 2013;154(5):1112-1126.

31. Varnum-Finney B, Halasz LM, Sun M, Gridley T, Radtke F, Bernstein ID. Notch2 governs the rate of generation of mouse long- and short-term repopulating stem cells. *J Clin Invest*. 2011;121(3):1207-1216.

32. Andersson ER, Sandberg R, Lendahl U. Notch signaling: simplicity in design, versatility in function. *Development*. 2011;138(17):3593-3612.

33. Palomero T, Sulis ML, Cortina M, et al. Mutational loss of PTEN induces resistance to NOTCH1 inhibition in T-cell leukemia. *Nat Med*. 2007;13(10):1203-1210.

34. Blank U, Karlsson G, Karlsson S. Signaling pathways governing stem-cell fate. *Blood*. 2008;111(2):492-503.

35. Pajcini KV, Speck NA, Pear WS. Notch signaling in mammalian hematopoietic stem cells. *Leukemia*. 2011;25(10):1525-1532.

36. Yao-Ming Ng S. YT, Zhang J., and Katia Georgopoulos. Genome-wide lineage-specific transcriptional networks underscore Ikaros-dependent lymphoid priming in hematopoietic stem cells. *Immunity*. 2009;30:493-507.

37. Doulatov S, Notta F, Eppert K, Nguyen LT, Ohashi PS, Dick JE. Revised map of the human progenitor hierarchy shows the origin of macrophages and dendritic cells in early lymphoid development. *Nat Immunol*. 2010;11(7):585-593.

FIGURE LEGENDS

Figure 1. Notch signaling maintains a CD45RA$^-$ cell subset in cultures of umbilical cord blood HSCs. A) Flow cytometric analysis of Lineage-depleted CD135$^+$. Three populations of CD45RA were observed (CD45RA$^-$, CD45RA^{int} and CD45RA^{hi}). CD45RA$^-$ were analyzed for CD133 expression and Rhodamine-1,2,3 (Rho) uptake which identified three levels of Rho staining (Rho^{low}, Rho^{int}, Rho^{hi}). The CD133$^+$Rho^{low} cells were analyzed for the expression of CD90 and CD135. CD90^{low} are referred to as HSC and CD90$^-$ cells are referred to as MPP. A representative experiment is shown from at least 10 independent analyses. B) Cocultures were initiated with CD90^{low} cells (HSCs) placed on OP9-Ctrl, -DL4^{hi} and -DL4^{low} cells and analyzed by flow cytometry at days 9, 16 and 21 of culture for the expression of CD34 as indicated. C) CD34$^+$ CD7$^-$ gated cells from the indicated co-cultures were analyzed at days 9, 16, and 21 for the expression of CD38 and CD45RA. Numbers within each plot indicate the percentage of cells in the indicated gates. A representative experiment is shown, from at least 10 independent cultures.

Figure 2. Notch signals lead to an enhanced cellular expansion of HSCs and CD45RA$^-$ cells with reconstitution potential in vivo. Cocultures were initiated with CD90^{low} cells (HSCs) placed on OP9-Ctrl, -DL4^{hi} and -DL4^{low} cells and analyzed by flow cytometry at days, 7, 14, and 21 of culture. The cellular fold expansion from the input number (5-10x10^3) is shown for (A) CD90^{low} and (B) CD45RA$^-$ cells. Bar graphs show mean and standard error of 6-8 independent experiments. Statistical significance is indicated as (*) for $p \leq 0.05$, and (**) for $p \leq 0.01$. Cocultures were initiated with HSCs placed on OP9-DL4^{hi} cells for 14 days, C) Phenotypically-defined pHSC/CD90^{low} and D) phenotypically defined pMPP/CD90$^-$ cells were isolated by flow cytometry, and 2x10^3 pHSC/CD90^{low} and 5x10^4 pMPP/CD90$^-$ cells were injected into sublethally irradiated NSG neonatal mice. Ten weeks after injection BM was analyzed by flow cytometry for the expression of the indicated marker. Numbers within each plot indicate the percentage of cells in the indicated gates or quadrants. E) Absolute numbers of CD14$^+$, CD15$^+$ and CD19$^+$ cells recovered. F) A linear correlation between the absolute numbers of

CD45RA$^-$ cells recovered from the BM and the number of freshly sorted HSCs injected into mice is shown (R^2=0.87). Absolute numbers of CD45RA$^-$ cells recovered from (C) and (D) were plotted on the linear graph and the corresponding number of HSCs injected was extrapolated. A total of 8 mice were analyzed.

Figure 3. ***In vitro, but not in vivo,*** **expansion of HSCs is Notch dependent.** A) Freshly sorted HSCs were transduced with dnMaml-GFP or control YFP-only retroviral constructs, and sorted on day 6 post-transduction as GFP$^+$ and YFP$^+$ cells, cultured on OP9-Ctrl, -DL4^{hi} -DL4^{low} cells for 2 weeks. Cultures were analyzed by flow cytometry for the expression of the indicated markers as shown for Total coculture. Cells gated as GFP$^+$ or YFP$^+$CD34$^+$CD7$^-$CD38$^-$ were further analyzed for the expression of CD45RA (34$^+$7$^-$38$^-$). Additionally, CD45RA$^-$ gated cells were analyzed for the expression of CD90 (34$^+$7$^-$38$^-$RA$^-$). Numbers within each plot indicate the percentage of cells in the indicated gates or quadrants. Representative plots from at least 3 independent experiments are shown. B) Cellular fold expansion of CD45RA$^-$ cells (5-10x10^3) is shown for the indicated coculture conditions at day 13 or 18 of culture relative to the start of coculture (i.e., following the initial 7d retroviral transduction period). Bar graphs show mean and standard error of 4 independent experiments. C) Freshly sorted HSCs were transduced with dnMaml-GFP or control YFP-only lentiviral constructs, and sorted on day 3 post-transduction as GFP$^+$ or YFP$^+$ CD34$^+$CD7$^-$CD38$^-$CD90^{low} (CD90^{low}) cells. Equal numbers of transduced GFP$^+$ or YFP$^+$ CD90^{low} cells were co-injected into sublethally irradiated NSG neonatal mice, and after ten weeks cells from the bone marrow were analyzed by flow cytometry for the indicated markers. C) Top rows indicate the frequency of donor cells in BM (CD45$^+$) and expression of GFP and YFP is shown for CD45$^+$-gated cells. Bottom rows show, GFP$^+$ and YFP$^+$ gated cells as indicated. Numbers within each plot indicate the percentage of cells in the indicated gates or quadrants. D) Absolute numbers of donor-derived CD90^{low} cells and (E) CD45RA$^-$ cells from the BM of host mice, as in C. A representative experiment is shown, from 3 reconstituted mice.

Figure 4. Notch signals lead to an enhanced cellular expansion of CD45RA^{-} cells and delay the cellular expansion of CD45RA^{int} and CD45RA^{hi} progenitors. Cocultures were initiated with CD90^{low} cells (HSCs) placed on OP9-Ctrl, -DL4^{hi} and -DL4^{low} cells and analyzed by flow cytometry at days, 7, 14, and 21 of culture. The cellular fold expansion based on the absolute numbers of cells recovered (from d0 5-10,000 HSC plated) is shown for CD45RA^{int} and CD45RA^{hi} cells (A). Bar graphs show mean and standard error of at least 10 independent experiments. B) Precursor-product relationship between CD45RA^{int} and CD45RA^{hi} cells. Cocultures were initiated with CD90^{low} cells (HSCs) placed on OP9-Ctrl, -DL4^{hi} and -DL4^{low} cells. After 21 days of culture, OP9-Ctrl, -DL4^{hi} and -DL4^{low} cultures were harvested separately and CD45RA$^{-/int}$ cells were sorted by flow cytometry and re-cultured under the same conditions in stem media. This defines a new d0 (purity analysis for this d0 shown). Two and three days later cells were analyzed for the expression of CD34 and CD45RA on gated CD34^{+}CD38^{-}CD7^{-} cells. Numbers within each plot indicate the percentage of cells in the indicated gates. Representative plots of 3 independent experiments are shown.

Figure 5. Lineage potential of CD45RA^{int} and CD45RA^{hi} cells. A) CFU-C generation from 500 plated, day 21 sorted CD45RA^{int} and CD45RA^{hi} cells, grown on OP9-DL4^{low} (1st panel) and/or OP9-Ctrl (2nd panel). CFU-C generation from *ex vivo* derived Stem, MPP and CD45RA^{int} Rho$^{low/int}$ CD133^{+}CD7^{-}CD10^{-} (*ex vivo* CD45RA^{int}) (3rd panel). Mean and standard error of the mean were calculated from 6 independent experiments. B) CFU-C generation from 1000 plated *ex vivo* CD90^{-} (MPP), CD45RA^{int} Rho^{int} cells or CD45RA^{int} Rho^{low} cells. C) Purity re-analysis of CD45RA^{int} d21 sorted fractions and *ex vivo* CD45RA^{int} is shown as d21 (+0d) (first column). Generation of CD5^{+}, CD7^{+} and CD1a^{+} cells is shown in the middle columns and CD19^{+} cells versus CD33^{+} in the last column for CD45RA^{int} derived from OP9-Ctrl and /or DL4^{low} and *ex vivo* CD45RA^{int}. D) Purity re-analysis of CD45RA^{hi} d21 sorted fractions is shown as d21 (+0d) (first column). Generation of T cells i*n vitro* by CD45RA^{hi} cells derived from OP9- Ctrl or OP9- DL4^{low} cultures is shown in the middle columns, and generation of CD19^{+} or CD33^{+} cells is shown in the last column. Numbers within each plot indicate the percentage of cells in the indicated gates. This is a representative experiment of at least 10 independent

experiments. E) *Ex vivo* CD90^{-} (MPP), CD45RA^{int} Rho^{int} cells or CD45RA^{int} Rho^{low} cells were cultured on OP9-Ctrl for 26 days and analyzed for the expression of CD34, CD10 and CD19 by flow cytometry. Numbers within each plot indicate the percentage of cells in the indicated gates

Figure 6. Profiling of CD45RA^{int} and CD45RA^{hi} cells: qPCR for transcripts expressed in CD45RA^{int} or CD45RA^{hi} derived from OP9- DL4^{low} or OP9- Ctrl and sorted on day 21. All samples were normalized to beta-actin. Mean and standard error of the mean were calculated from 3-5 independent qPCR analyses.

Figure 7. In vivo differentiation potential of CD45RA subsets: Sublethally irradiated immune-deficient neonates were injected with *in vitro* derived or *ex vivo* derived indicated cells at concentrations ranging from 0.1-1x10^{5} cells/mouse. After 4-7 weeks, mice were sacrificed and thymi and/or bone marrow cells were analyzed by flow cytometry for shown markers. A, D) Percent donor CD45^{+} cells in BM and/or thymus from mice injected with CD45RA^{int} derived from OP9-DL4^{low} or OP9-Ctrl cultures (15 and 7 mice respectively) B, D) Percent CD45^{+} marker positive cells found in BM and/or thymus of mice injected with CD45RA^{hi} derived from OP9-DL4^{low} or OP9-Ctrl cultures (5 and 4 mice respectively) or C, D) *ex vivo* CD45RA^{int} (7-8 mice).

Figure 1

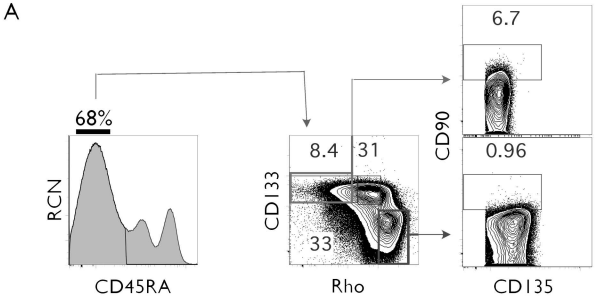
A
68%
RCN
CD45RA
8.4
31
33
CD133
Rho
6.7
0.96
CD90
CD135

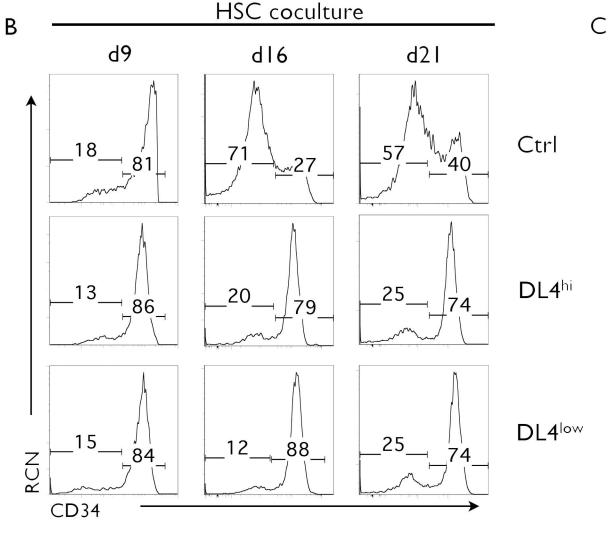
B
HSC coculture
d9
d16
d21
18
81
71
27
57
40
Ctrl
13
86
20
79
25
74
DL4hi
15
84
12
88
25
74
DL4low
RCN
CD34

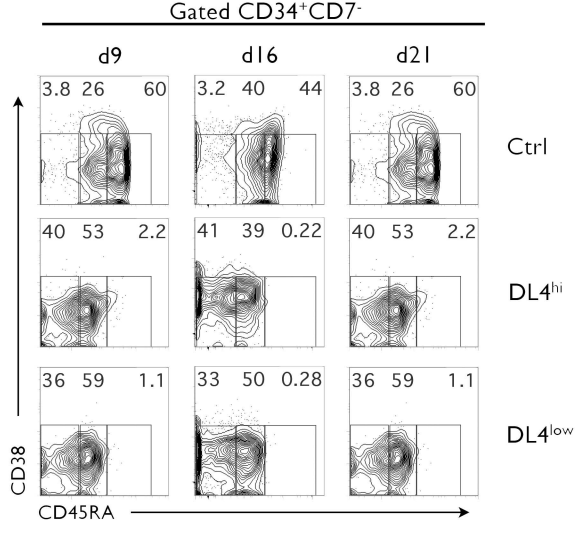
C
Gated CD34+CD7-
d9
d16
d21
3.8 26 60
3.2 40 44
3.8 26 60
Ctrl
40 53 2.2
41 39 0.22
40 53 2.2
DL4hi
36 59 1.1
33 50 0.28
36 59 1.1
DL4low
CD38
CD45RA

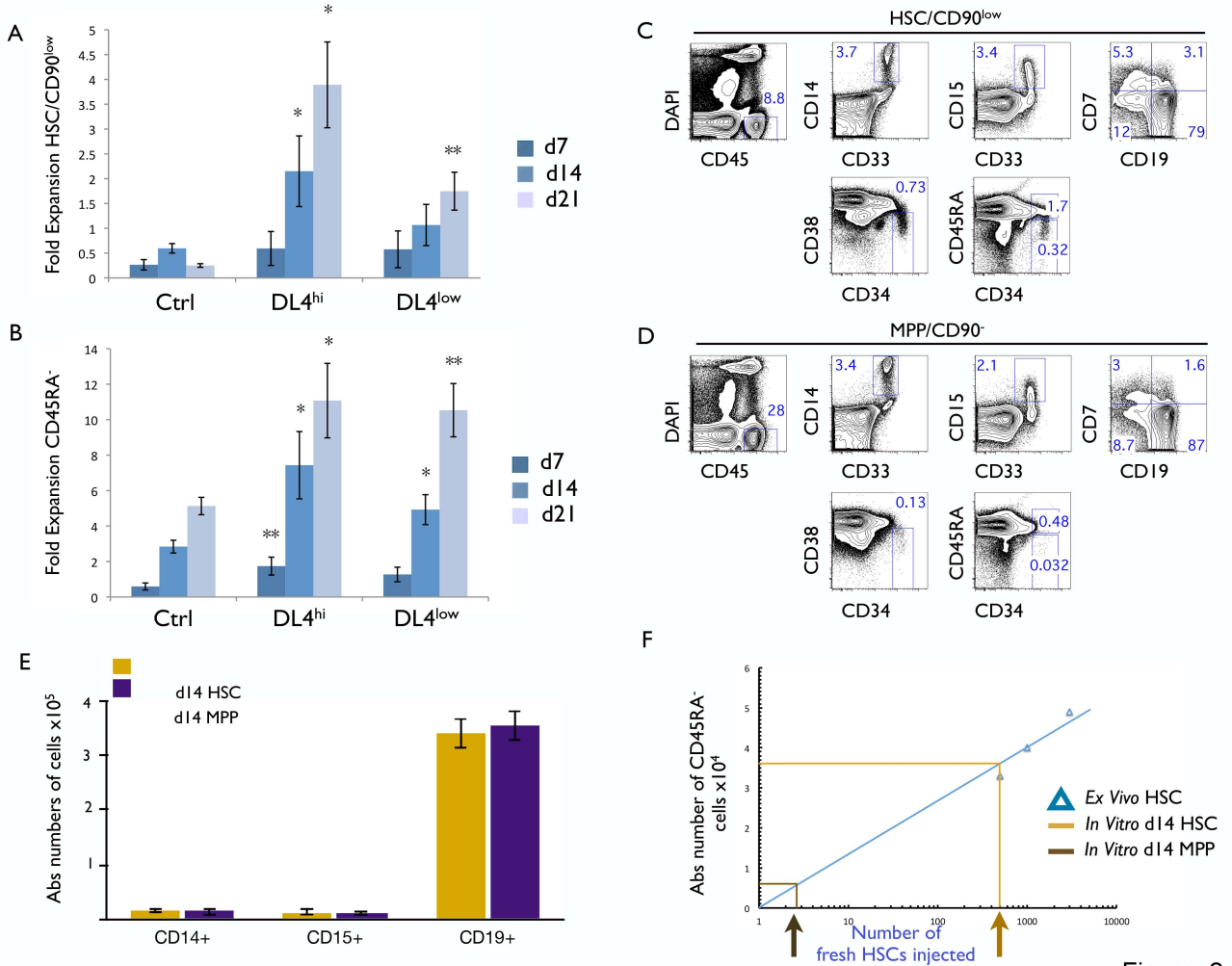
A
Fold Expansion HSC/CD90low
d7
d14
d21
Ctrl
DL4hi
DL4low
B
Fold Expansion CD45RA-
C
HSC/CD90low
DAPI
CD45
CD14
CD33
CD15
CD33
CD7
CD19
CD38
CD34
CD45RA
CD34
D
MPP/CD90-
E
d14 HSC
d14 MPP
Abs numbers of cells x10^5
CD14+
CD15+
CD19+
F
Abs number of CD45RA- cells x10^4
Ex Vivo HSC
In Vitro d14 HSC
In Vitro d14 MPP
Number of fresh HSCs injected

Figure 2

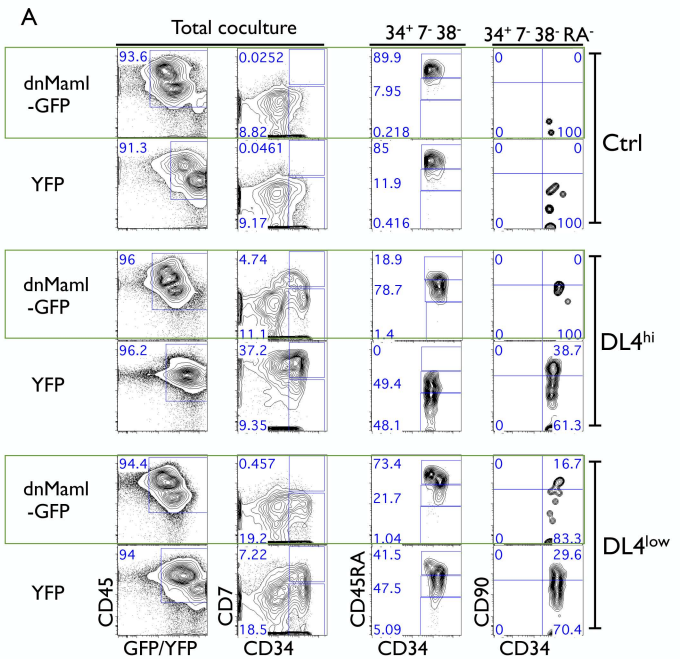
A
Total coculture
34+ 7- 38-
34+ 7- 38- RA-
dnMaml -GFP
YFP
Ctrl
DL4hi
DL4low
CD45
GFP/YFP
CD7
CD34
CD45RA
CD90

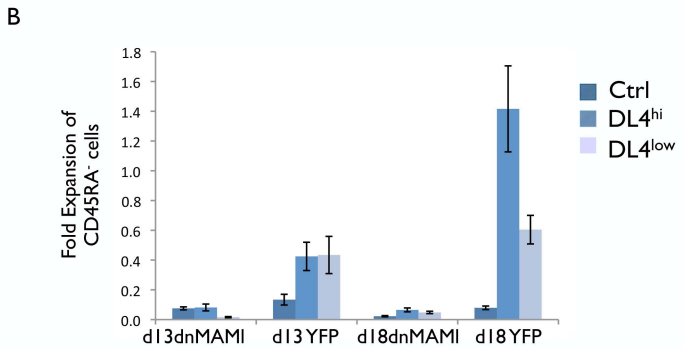
B
Fold Expansion of CD45RA- cells
Ctrl
DL4hi
DL4low
d13dnMAMl
d13YFP
d18dnMAMl
d18YFP

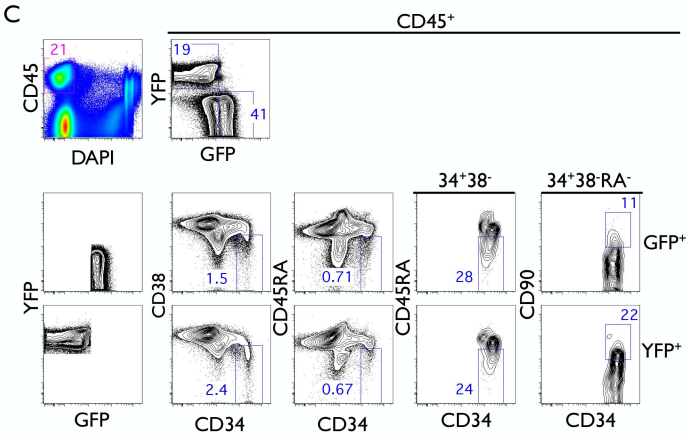
C
CD45+
CD45
DAPI
YFP
GFP
34+38-
34+38-RA-
CD38
CD45RA
CD90
CD34
GFP+
YFP+

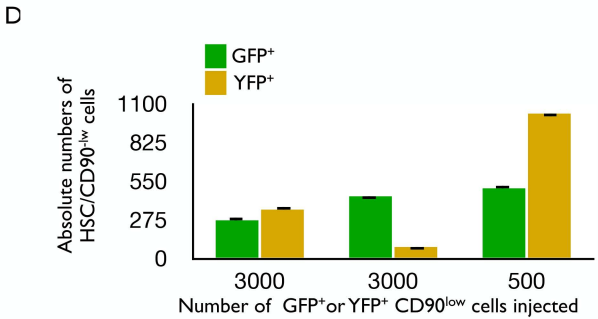
D
GFP+
YFP+
Absolute numbers of HSC/CD90-lw cells
Number of GFP+or YFP+ CD90low cells injected

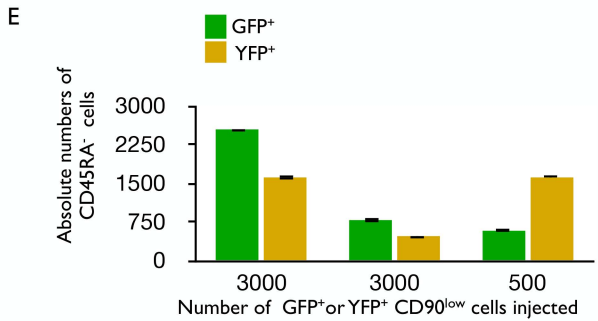
E
GFP+
YFP+
Absolute numbers of CD45RA- cells
Number of GFP+or YFP+ CD90low cells injected

Figure 3

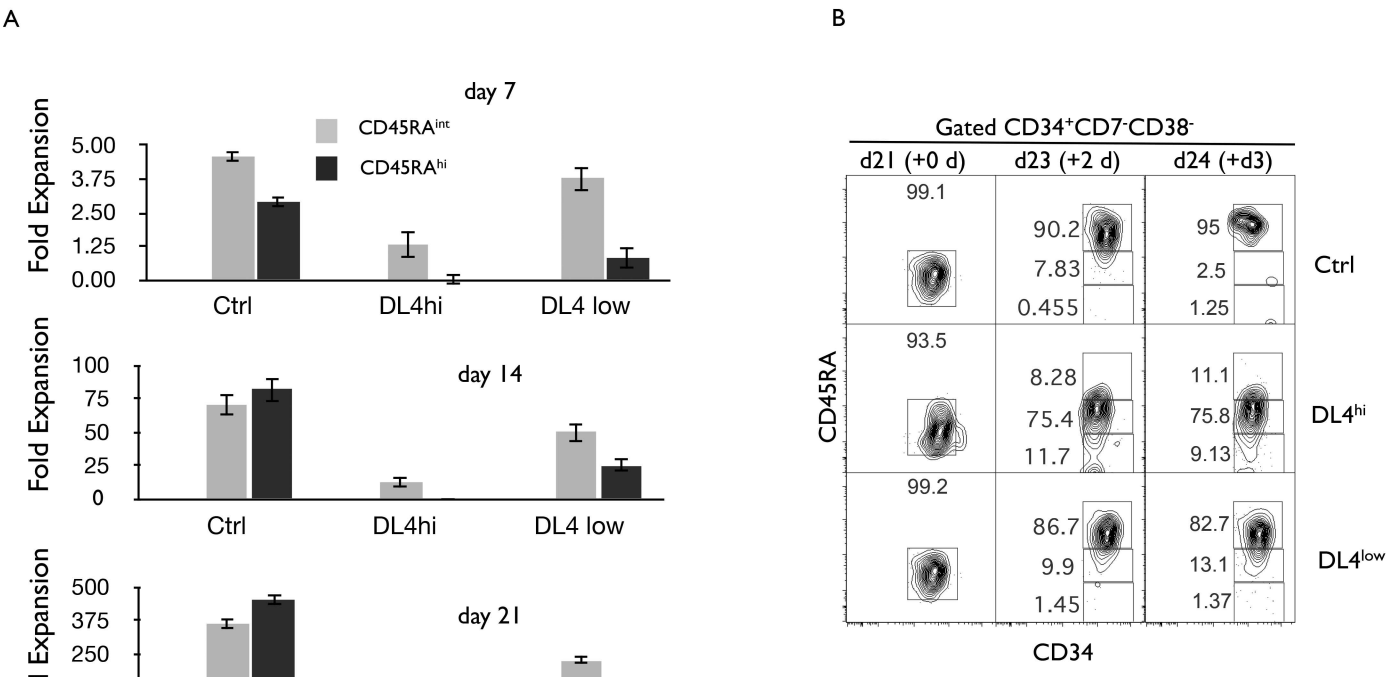
A
day 7
CD45RA^int
CD45RA^hi
Fold Expansion
5.00
3.75
2.50
1.25
0.00
Ctrl
DL4hi
DL4 low
day 14
100
75
50
25
0
day 21
500
375
250
125
B
Gated CD34+CD7-CD38-
d21 (+0 d)
d23 (+2 d)
d24 (+d3)
99.1
90.2
7.83
0.455
95
2.5
1.25
Ctrl
93.5
8.28
75.4
11.7
11.1
75.8
9.13
DL4hi
99.2
86.7
9.9
1.45
82.7
13.1
1.37
DL4low
CD45RA
CD34

Figure 4

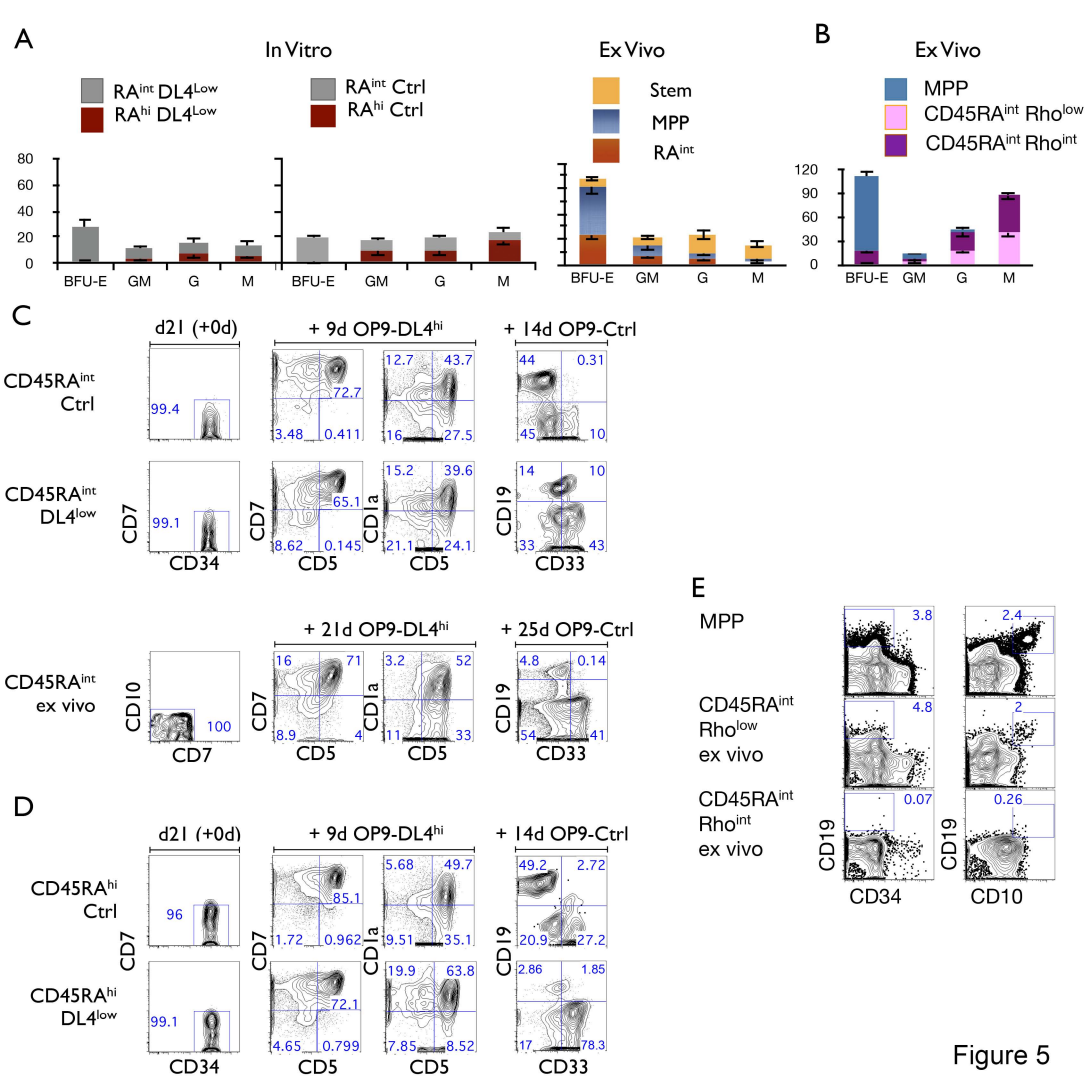
A
In Vitro
RA^int DL4^Low
RA^hi DL4^Low
RA^int Ctrl
RA^hi Ctrl
Ex Vivo
Stem
MPP
RA^int
BFU-E
GM
G
M
B
Ex Vivo
MPP
CD45RA^int Rho^low
CD45RA^int Rho^int
C
d21 (+0d)
+ 9d OP9-DL4^hi
+ 14d OP9-Ctrl
CD45RA^int Ctrl
CD45RA^int DL4^low
CD7
CD34
CD5
CD1a
CD19
CD33
+ 21d OP9-DL4^hi
+ 25d OP9-Ctrl
CD45RA^int ex vivo
CD10
D
CD45RA^hi Ctrl
CD45RA^hi DL4^low
E
MPP
CD45RA^int Rho^low ex vivo
CD45RA^int Rho^int ex vivo

Figure 5

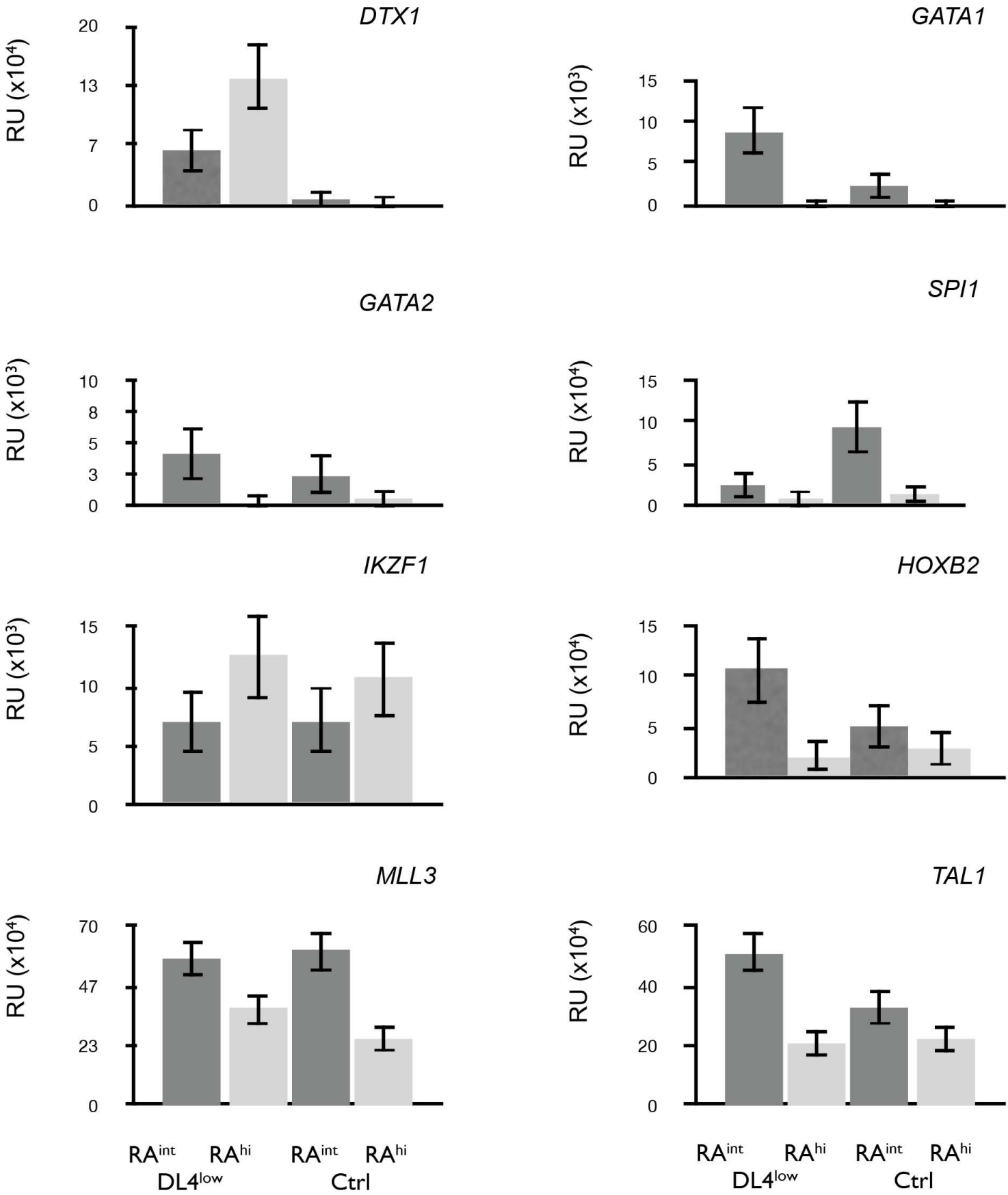
DTX1
RU (x10⁴)
20
13
7
0
GATA1
RU (x10³)
15
10
5
0
GATA2
RU (x10³)
10
8
5
3
0
SPI1
RU (x10⁴)
15
10
5
0
IKZF1
RU (x10³)
15
10
5
0
HOXB2
RU (x10⁴)
15
10
5
0
MLL3
RU (x10⁴)
70
47
23
0
TAL1
RU (x10⁴)
60
40
20
0
RA^int RA^hi RA^int RA^hi
DL4^low Ctrl
RA^int RA^hi RA^int RA^hi
DL4^low Ctrl

Figure 6

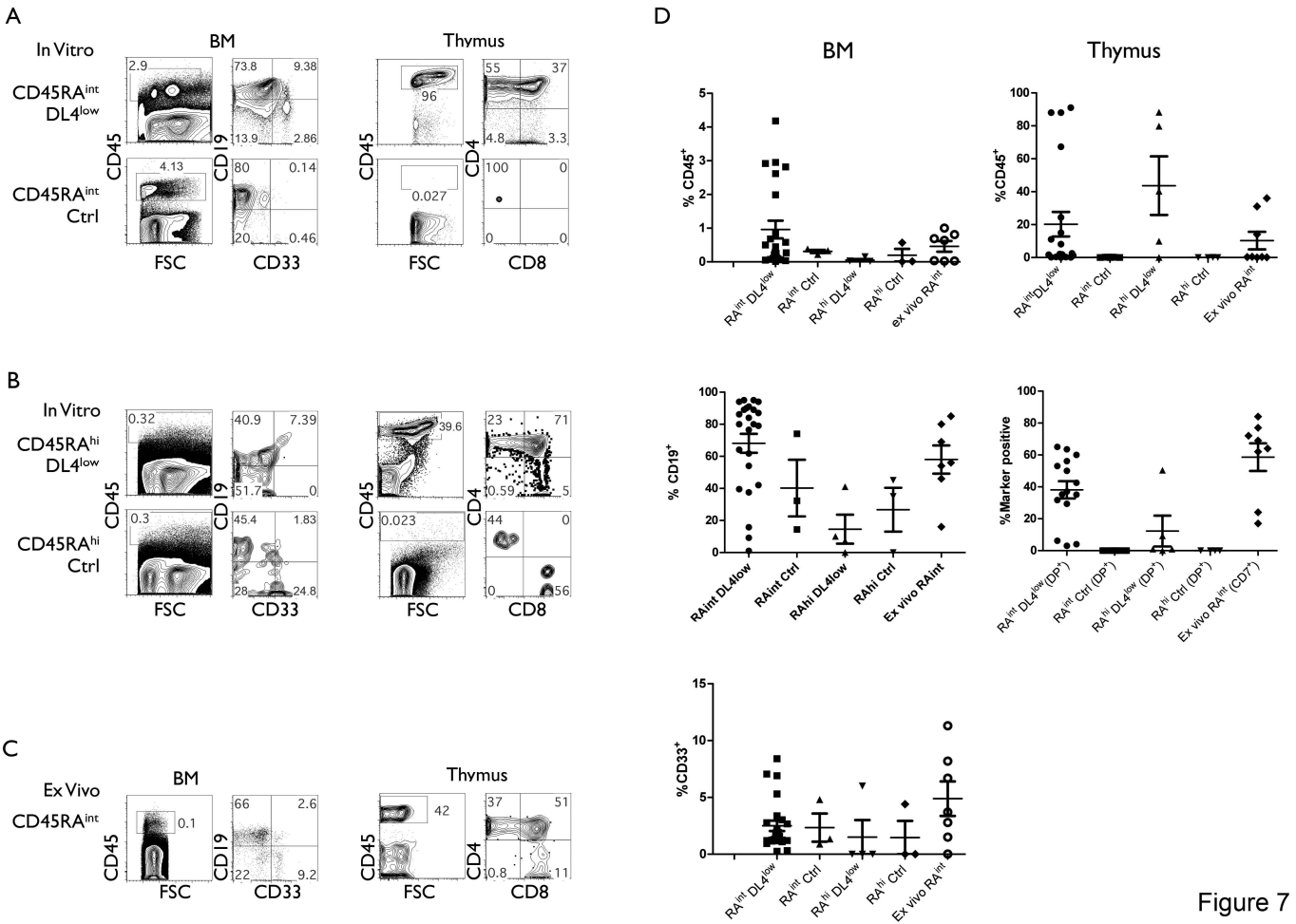
A
In Vitro
BM
Thymus
CD45RA^int DL4^low
CD45RA^int Ctrl
CD45
CD19
CD33
CD4
CD8
FSC
2.9
73.8
9.38
13.9
2.86
4.13
80
0.14
20
0.46
96
55
37
4.8
3.3
0.027
100
0
0
0
B
In Vitro
CD45RA^hi DL4^low
CD45RA^hi Ctrl
0.32
40.9
7.39
51.7
0
0.3
45.4
1.83
28
24.8
39.6
23
71
10.59
5
0.023
44
0
10
56
C
Ex Vivo
CD45RA^int
0.1
66
2.6
22
9.2
42
37
51
10.8
11
D
BM
Thymus
% CD45+
% CD19+
%CD33+
%Marker positive
RA^int DL4^low
RA^int Ctrl
RA^hi DL4^low
RA^hi Ctrl
ex vivo RA^int
Ex vivo RA^int
RAint DL4low
RAint Ctrl
RAhi DL4low
RAhi Ctrl
Ex vivo RAint
RA^int DL4^low (DP+)
RA^int Ctrl (DP+)
RA^hi DL4^low (DP+)
RA^hi Ctrl (DP+)
Ex vivo RA^int (CD7+)

Figure 7